ECRF stray radiation studies in preparation of the operations of JT-60SA

Carlo Sozzi[1*], *Ken* Kajiwara[2], *Takayuki* Kobayashi[2], *Lorenzo* Figini [1], *Luca* Garzotti[3], *Alessandro* Moro[1], *Silvana* Nowak[1], *David* Taylor[3].

[1]Institute for Plasma Science and Technology (ISTP-CNR), Italy
[2]National Institutes for Quantum and Radiological Science and Technology, QST, Naka, Ibaraki 311-0193, Japan
[3]CCFE, Culham Science Centre, Abingdon, UK

Abstract. JT-60SA tokamak is equipped with an ECRF system since the beginning of its operational phase. Starting from two gyrotrons units during the Integrated Commissioning, applicable for core heating, assisted breakdown and assisted Wall Conditioning, the system capabilities will be progressively extended from the Initial Research phase for wider applications. The development of the full current plasma H mode scenario 2 (inductive, type I ELM, I_p=5.5 MA, B_T=2.25 T, q_{95}=3) is among the first scientific objectives of the research program. In preparation of this, predictive modelling of the current ramp-up in scaled versions of scenario 2 is being done, based on parameters previously published. In this scenario the ECRF power is injected from an early phase of the discharge. Such modelling provides the kinetic profiles giving the opportunity to estimate the expected amount of EC stray radiation during the ramp-up phase when the EC power absorption might be less than 100% and consequently the potential risk of damage of the in-vessel components is higher.

1 Introduction

JT-60SA is the large superconducting tokamak built under the Broader Approach agreement jointly by Europe and Japan [1] and now under its commissioning phase. It is designed to address many areas of fusion science in preparation of the burning plasma era of ITER and DEMO, in particular the ones related with the control of high β steady state plasmas and the confinement of high energy particles. Several different main operation scenarios (plus variants) are foreseen for JT-60SA [1, 2, 3] in the research phases, with toroidal magnetic field of 2.25-2.28 T (inductive scenarios) and 1.62-1.72 T (non-inductive).

At its full development, the ECRF system is designed for 9 gyrotrons able to inject up to 7 MW to the plasma from 4 toroidally distributed upper oblique launchers with extended poloidal and toroidal steering capability and pulse duration up to 100 s. Each gyrotron can provide EC power at three different frequencies, namely 82, 110 and 138 GHz [4, 5]. Before full performance will be made available, gradually increasing capabilities are foreseen for the Integrated Commissioning (IC) phase (~2023) and for the Initial Research phase (IR, ~2025-2026).

For the IC 2 gyrotron of about 1 MW power each (at source) are available, one at fixed 110 GHz frequency, and one at selectable frequency of 82, 110 and 138 GHz. In the latter, the maximum power depends on the selected frequency (1.5 MW at 110 GHz, 0.75 at 138 and 0.6 at 82). The two gyrotrons have separated power supplies and then can be pulsed with different waveforms, in particular at different starting times. In the IC the ECRF power is launched with a fixed angle two-waveguide launcher parallel to the port axis (and perpendicular to the toroidal field) at 35.5° with respect to the equatorial plane. Both X and O polarization (and their combinations) are available. The ECRF pulse duration is up to 5 sec for 110 and 138 GHz and up to 1 sec for 82 GHz. The launching settings available during the IC, with beam injection towards the centre of the vessel, allow the application of the ECRF power for core heating, ECRF assisted breakdown and ECRF assisted Wall Conditioning.

For its IR phase, the JT-60SA tokamak will be equipped with four gyrotrons units delivering a maximum of 3 MW at 110 GHz to the plasma, or 1.5 MW at 110 GHz plus 1.5 MW at 138 GHz. The available additional power also includes 6 MW of P-NBI and 10 MW of N-NBI.

The development of the so-called scenario 2 (inductive H mode scenario, lower single null CFC divertor plasma configuration, type I ELMs, I_p=5.5 MA, B_T=2.25 T, q_{95}=3) is among the first scientific objectives of the IR phase. In preparation of this goal, predictive modelling of the current ramp-up is being performed. This was first analysed with a fast integrated tokamak modelling tool (METIS+FEEQS) in [6]. A similar current ramp-up in fully predictive way was simulated using the JINTRAC suite of codes [7]. In these simulations the plasma current evolution was imposed as boundary condition, the equilibrium was calculated

* Corresponding author: carlo.sozzi@istp.cnr.it

with the ESCO equilibrium solver and updated periodically throughout the simulation. The transport model adopted for the simulation is the Bohm/gyro-Bohm transport model. The density was controlled by a numerical feed-back mechanisms adjusting the prescribed gas puff to deliver the required density ramp. The power deposition was calculated with GRAY (ECRF) and PENCIL (NBI) [7].

Safe approach to operations at full plasma current suggests a gradual development path to reach the full performance scenario, like the one described in the JT-60SA Research Plan [1]. For this purpose, variations of scenario 2 at reduced plasma current and magnetic field are being considered in this paper. In particular a range of ramp-up cases are analysed. The ECRF power is injected from an early phase of the discharge when the EC power absorption is generally less than 100%. Consequently, the potential risk of damage of the in-vessel components may be higher. The JINTRAC modelling provides T_e ad n_e profiles from which is possible to estimate the expected EC absorption and, conversely, the amount of EC stray radiation during the ramp-up. Fixed ECRF launching settings are assumed, with the beams directed towards the plasma core. Such launching settings are representative either of the basic configuration for core heating in the IR phase and of the one available during the IC phase.

In all the cases except one the rise of the plasma current is limited to 2.1 MA. For the IC plasma currents ranging from few hundred kA up to about 2.5 MA [8] are being considered in single null configuration with the X-point close to the top of the vessel. However, since the absorption and beam trajectory mainly depend on plasma temperature and density in the plasma core, the results here obtained for the reduced scenario 2 are also relevant for the IC provided that similar axial density and temperature are realized.

The study of the current ramp-up phase complements the analysis of the low absorption scenarios being considered for the design of the EC stray detection system for the IR phase [9]. To this purpose, the adaptation to the JT-60SA parameters of the differential bolometers being developed for ITER is in progress. No direct measurements of the EC stray radiation are available in the IC.

The expected EC stray power loads on PFCs due to shine-through of the EC beams for some specific case is also reported in the paper.

2 Heating scenarios during the plasma current ramp-up

One possible option for the development of a plasma scenario up to full performance is the progressive increase of the flat top plasma current and of the toroidal field while keeping constant the edge safety factor q_{95}. This approach is motivated by the opportunity of minimizing the operation risks related to high plasma current while keeping similar magnetic equilibria and plasma shape, also reducing the amount of additional heating needed to sustain the scenario.

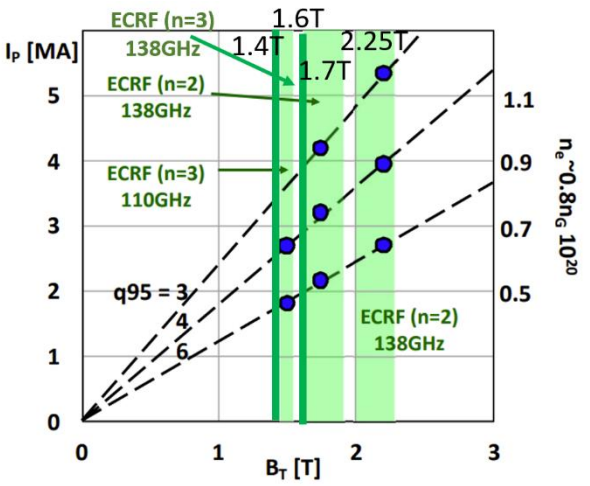

Fig. 1. Possible operational path for the rise to 5.5MA in the Initial Research phase. Adapted from [1]

Alternatively, the plasma current can be increased at a given toroidal field progressively lowering the q_{95}. The range of possible I_p, B_T, EC frequency combinations that allow the use of the ECRF heating is shown Fig. 1 for three values of q_{95}.

Table 1. ECRF heating cases during the current ramp-up

case	B_T [T]	Ip [MA]	Te [keV]	n_e [10^{19} m^{-3}]	t[s]	Injected P_{EC} [MW]
1a	2.25	0.81	0.55	0.81	2.9	0.5
1b	2.25	2.86	6.7	1.18	8.3	3.5
1c	2.25	5.5	10	3.1	15	7
2a	2	2.1	1.55	1.6	8.2	0.75
2b	2	2.1	3.32	1.75	9.2	1.5
3	2	2.1	1.57	1.61	8.2	1.5
4a	1.8	1.08	0.56	0.9	3.3	0.215
4b	1.8	1.9	1.31	1.07	5.3	0.428
4c	1.8	2.1	2.33	1.6	8.3	0.75
5a	1.8	2.1	1.52	1.58	8.2	0.75
5b	1.8	2.1	2.85	1.74	9.2	1.5
6a	1.7	2.1	1.37	1.5	8.25	0.75
6b	1.7	2.1	2.27	1.87	9.3	1.5
7	1.7	2.1	1.32	1.5	8.2	1.5
8	1.6	2.1	1.6	1.7	8.2	0.75
9a	1.4	1.06	0.41	1.2	3.3	0.215
9b	1.4	1.92	1.07	1.17	5.3	0.428
9c	1.4	2.1	1.39	1.67	8.3	0.75

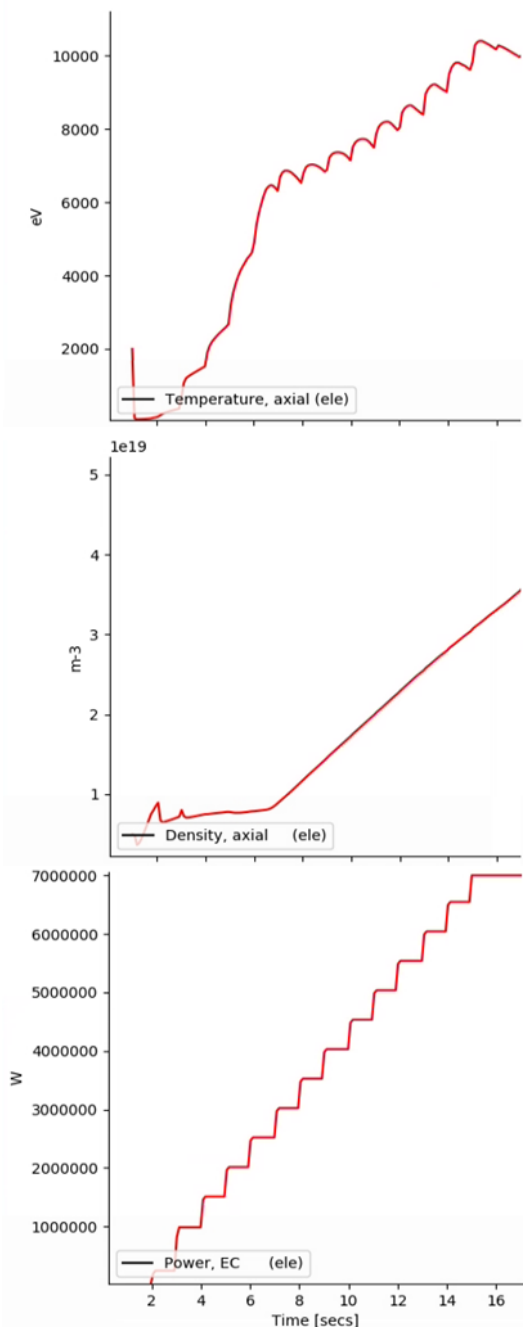

Fig. 2. Time evolution of the axial electron temperature (top), of the axial density (mid) and of the absorbed EC power (bottom) for case 1 simulation in Table 1.

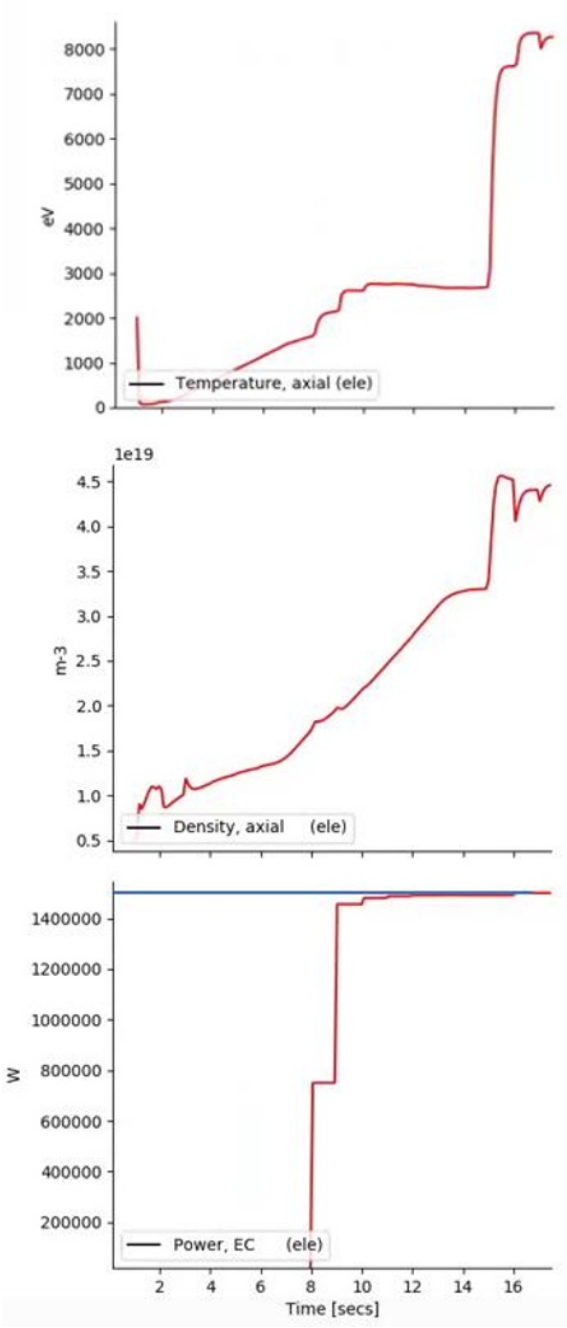

Fig. 3. Time evolution of the axial electron temperature (top), of the axial density (mid) and of the absorbed EC power (bottom) for case 6 simulation in Table 1.

A reduced subset of heating cases in current ramp-up is listed in Table 1 in which the main parameters at the time and radial location of the ECRF injection are listed, along with the power at the corresponding time.

The case label (first left column) corresponds to a given simulation run (1,2…) at different times (a,b,…). Cases 1, 4 and 9 are power ramps with injection starting 2 s after the breakdown (see Fig. 2), while the others are power steps with injection starting at 8 s (see Fig. 3).

During the ramp-up of the discharge ECRF is the only active additional heating system.

Case 1 refers to the nominal scenario 2 at full current (5.5 MA) and full ECRF power (7 MW to the plasma). The time evolution of the electron temperature, of the density at the magnetic axis and of the absorbed ECRF power is shown in Fig. 2. In all the other cases 2-9, the power of one or two gyrotrons only is considered. For these cases the current ramp ends at 6 s, then in cases 2, 3, 5, 6, 7 and 8 the injection occurs 1 in 1 or 2 power steps, separated by 1 s, at the beginning of the current flat top during the rise of the density and of the temperature as shown in Fig. 3 for case 6. The sudden rise of density and temperature at a later time in the simulation (15 s) with respect to the ECRF power steps is related with the switch on of the Neutral Beam power which is not discussed in this paper. The effect of the ECRF power is visible in density and temperature time

traces. The resonance layers for the two EC frequencies in this case are located at 20-30% of the minor radius.

In cases 4 and 9 the ECRF injection starts in the early phase of the current ramp, at a temperature of few hundred eV and density of about $1 \cdot 10^{19}$.

In some cases (4, 5, 6, 7, 9) two different EC frequencies are injected, 110 and 138 GHz. The combination of two different frequencies provides some flexibility in the heating radial profile prior of the availability of the steerable ECRF antenna.

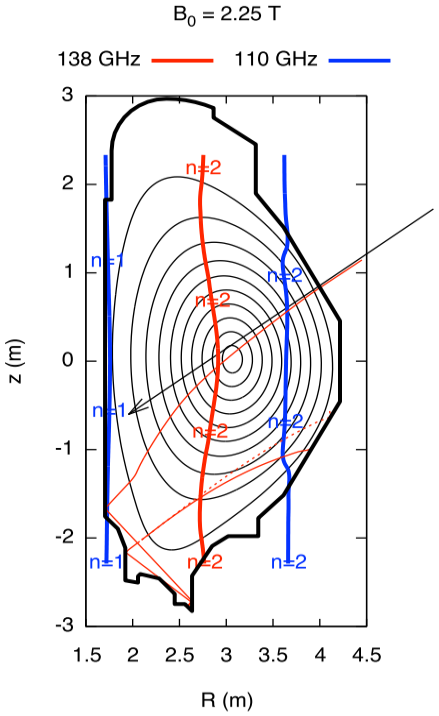

Fig. 4. Beam trajectory (red lines) and EC resonances for the harmonic n for scenario 2 at nominal magnetic field. The black arrow represents the initial injection direction. Applies to case 1.

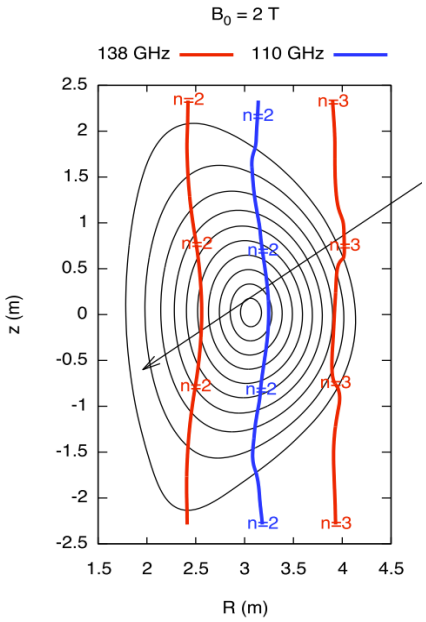

Fig. 5. EC resonances for B_0=2T (cases 2, 3).

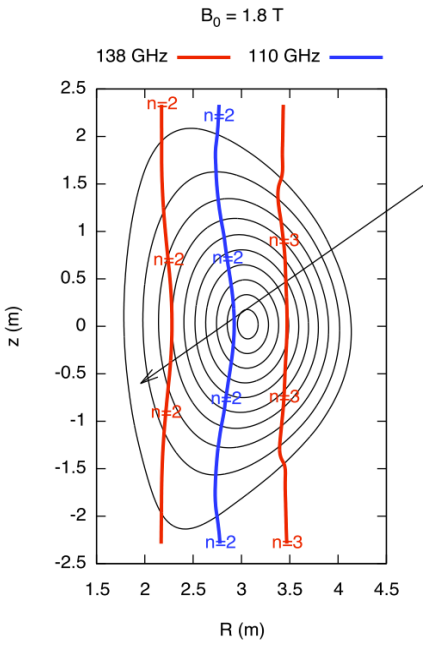

Fig. 6. EC resonances for B_0=1.8T (cases 4, 5)

Example applications in which this may be used is for extending the volume of the region of EC assisted breakdown, or for tailoring the current profile during the ramp.

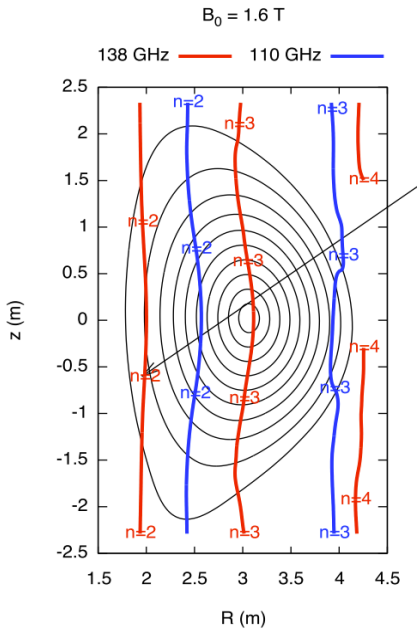

Fig. 7. EC resonances for B_0=1.6 T (case 8).

Figures 4-8 show the position of the EC resonances for harmonics n=2,3,4, X polarization, for both 110 GHz and 138GHz frequencies for the heating scenarios of Table 1. In all the cases the beam is launched towards the plasma centre (-35.5° with respect to the horizontal plane). Fig. 4 also shows the beam trajectory computed for the reference scenario (volume averaged electron temperature and density respectively 6.3 keV and 0.56 $10^{20}/m^3$ in the current flat top). The beam trajectory is

extended showing the reflection points in the vessel in the case in which the absorption is not total.

In some of the heating scenarios (e.g. Figures 5 and 7) absorption layers enter the outer region of the plasma, either in the low or high field side, resulting in the broadening of the absorption region and in the depletion of the power delivered to the plasma centre. This is for example visible in Fig. 9 that shows density (top), temperature (mid) and power deposition profiles (bottom) for case 6b, where the appearance of the 2nd harmonic absorption layer at the plasma edge subtracts power to the 3rd harmonics absorption layer in the plasma centre. This occurs to a much lesser extents when the edge absorption layer is of a higher harmonic as for example cases 2 and 3 in Fig. 5. However, higher harmonic outer absorption may become detrimental when the scenario is fully developed and the pedestal temperature increases. In the ramp-up cases here discussed, third harmonics absorption become effective, and apparent in the power deposition profile, when the temperature at the absorption region is above ~1 keV.

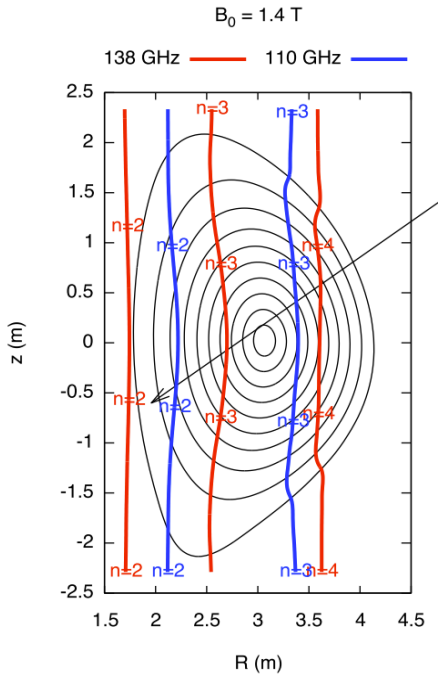

Fig. 8. EC resonances for B_0=1.4T (case 9)

3 Evaluation of the stray EC radiation

The results of the simulations for what concerns the evaluation of the EC stray radiation are summarized in Table 2 for the same cases listed in Table 1. For each heating case, along with the EC frequencies and harmonics, the position of the absorption layer, the percentual absorption (abs%) and the corresponding amount of EC stray power (P_{EC} stray) are listed in the two last right-hand columns. The absorption is evaluated at the time of the switch on assuming perfect matching of the polarization of the injected beam (100% X in this case). The amount of EC stray power (last right column) is estimated as follows. For the given value of the non

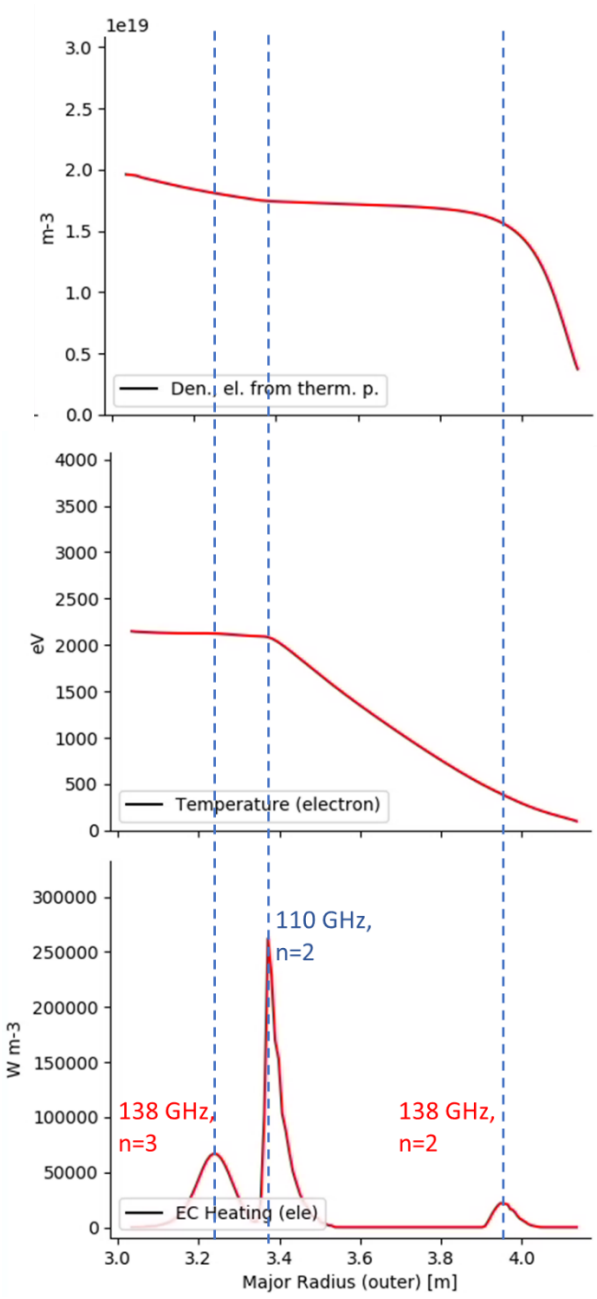

Fig. 9. Density, temperature and absorption profiles for case 6b

absorbed power as for column abs%, a further amount is added. This takes into account 5% of spurious cross-polarized component with respect to the main (X) polarization. This is a conservative, reference value from literature, justified by the effect of High Orders Modes [10] in the transmission line and by cross-polarization scattering due to turbulent fluctuations in the tokamak edge [11]. Within the range of the studied cases, relatively low values of absorption occur for injection times before about 5 s when the temperature is about 1 KeV or less (cases 1a, 4a, 4b, 9a, 9b) and when 3rd harmonic is used without a sufficiently long period of 2nd harmonic pre-heating. This can be seen for example comparing cases 6b and 7, with respectively 97% and 93.3% of absorption, that only differ for the time of the 3rd harmonic switch-on with respect to the

2nd harmonic (simultaneous in case 7). In all the other cases (10 out of 18) the absorption is higher than 99%. Only 4 cases out of 18 have absorption minor than 90%.

Non absorbed EC radiation may cause additional thermal load on specific locations of the first wall or in other components exposed to the EC waves, in particular in the area in front of the ECRF launchers. The beam propagation in cases of low plasma absorption has been studied for the steerable launchers in [12] using a realistic antenna modelling [4, 13].

Table 2. EC power stray for the cases of Table 1. Symbol (…) in the R_{abs} means that the absorption corresponding to the frequency and harmonic is negligible

case	f_{EC}[Ghz](N)	R_{abs} [m]	abs%	P_{EC} stray [kW]
1a	138(2)	3.31	48.30	261.00
1b	138(2)	3.29	>99	17.50
1c	138(2)	3.06	>99	35.00
2a	110(2)	3.15	>99	3.75
2b	110(2)	3.17	>99	7.50
3	110(2)	3.15	>99	7.50
4a	110(2) +138(3) +138(2)	3.30+ (...)+ 3.84	69.77	66.08
4b	110(2) +138(3) +138(2)	3.26 +(...) +3.82	92.10	35.95
4c	110(2) +138(3) +138(2)	3.23 +3.42 +3.83	99.07	10.75
5a	110(2)	3.21	>99	3.75
5b	110(2) +138(3) +138(2)	3.23 +3.43 +3.85	99.56	14.16
6a	110(2)	3.35+	>99	3.75
6b	110(2) +138(3) +138(2)	3.37 +3.24 +3.95	97.00	52.50
7	110(2) +138(3) +138(2)	3.36 +3.23 +3.94	93.33	107.50
8	138(3) +138(2)	3.02 +4.04	62.14	287.73
9a	110(3) +138(3) +110(2)	3.24 +3.24 +3.88	50.29	107.96
9b	110(3) +138(3) +110(2)	3.29 +3.29 +3.85	91.06	40.39
9c	110(3) +138(3) +110(2)	3.40 +3.40 +3.85	99.93	4.29

The peak power density incident in and the peak absorbed power by the plasma facing components corresponding to the aforementioned cross-polarization are summarized in Table 3 where the EC stray load due to the residual cross polarized component (OM2) at launch is reported. This unwanted component is partially transmitted through the plasma even at relatively high plasma temperature. The range 0-8 keV has been considered using beam tracing [12] and values for 5 keV temperature are listed for reference in the table. Depending on the plasma parameters and on the position in the vessel this effect may lead to relatively localized power deposition in the range of 3-50 kW/m^2.

Table 3. Residual cross polarized fraction (5%) at 5 keV plasma temperature for scenario 2, 138 GHz. Estimated per 1 MW power injected beam

(kW/m^2)	peak incident power density		peak absorbed power density on CFC		dura-tion
poloidal angle	bounce		bounce		
	1st	2nd	1st	2nd	
-35.5	334.5	41.4	29.8	3.7	pulse length

Similarly, Table 4 summarizes the same quantities for the case of a plasma having low absorption characteristics, as for example at the start-up. Values in the table corresponds to a plasma with 50 eV central temperature. A more extensive analysis for a range of ECRF launching settings and plasma parameters is reported in [12]. Specific evaluations for the launching settings of the IC phase are instead reported in [9]. The last column of Tables 3 and 4 contain an indication of the duration of the conditions causing the EC stray effect. For the cross-polarization case such effect is expected to last for all the duration of the ECRF heating. The EC stray due to the low absorption phase is expected to last from few ms to 2 s, and it can in any case be limited setting an appropriated control loop within the Plasma Control System.

Table 4. Low absorption phase scenario 2, 138 GHz at low plasma temperature (50 eV). Estimated per 1 MW power injected beam

(kW/m^2)	peak incident power density		peak absorbed power density on CFC		dura-tion
poloidal angle	bounce		bounce		
	1st	2nd	1st	2nd	
-35.5	669	0.28	59.54	0.02	1-2000 ms

4 Summary and perspectives

In this work we address the application of ECRF during the ramp-up of the plasma current and the early phase of the current flat top, with fixed ECRF launching settings, assuming a few hypothetical plasma scenarios scaled from the reference scenario 2. Since the absorption and beam trajectory in this early phase of the discharge mainly depend on plasma temperature and density, the results are relevant for both the IC and for the development of scenario 2 in IR.

This paper is a starting point in the exploration of the application of ECRF during the ramp-up from the standpoint of ECRF operation and in particular for what concerns the EC stray power. The reported results indicate good perspectives for the use of ECRF also in plasma scenarios with reduced magnetic field according with the development path described in the JT-60SA Research Plan.

Use of mixed ECRF frequencies at different harmonic, typically 110Ghz n=2+138Ghz n=3, appears feasible with the caveat that the absorption of the 3rd harmonic is favored by pre-heating with the second one.

An extension of the present analysis will include a wider range of the start-up times of the ECRF and of the launching settings keeping into account the steering capabilities of the ECRF launcher after the Integrated Commissioning phase.

This work has been carried out within the framework of the EUROfusion Consortium, funded by the European Union via the Euratom Research and Training Programme (Grant Agreement No 101052200 - EUROfusion). Views and opinions expressed are however those of the author(s) only and do not necessarily reflect those of the European Union or the European Commission. Neither the European Union nor the European Commission can be held responsible for them.

References

1. JT-60SA Research Unit, JT-60SA Research Plan, Version 4.0, September 2018, *http://www.jt60sa.org/pdfs/JT-60SA_Res_Plan.pdf* Chapter 3, “Operation Regime Development”
2. L. Garzotti et al., Nucl. Fusion 58 026029 (2018)
3. M Yoshida et al 2022 Plasma Phys. Control. Fusion 64 054004
4. T. Kobayashi et al., Fusion Engineering and Design 96–97 (2015)
5. T. Kobayashi et al., Nucl. Fusion 62 026039 (2022)
6. V. Ostuni et al., Nucl. Fusion 61 026021 (2021)
7. L. Garzotti et al., report SA-SE.CM.M.02-T001-D001 EFDA_D_2P4FS5, 2021 (private communication)
8. Y. Kamada et al., Nucl. Fusion 62 042002 (2022)
9. A. Moro et al, Proc. Of SOFT Conference 2022
10. E. Kowalski et al., IEEE Transactions on Microwave Theory and Techniques Vol. 58, Oct 2010
11. L. Guidi et al 2016 J. Phys.: Conf. Ser. 775 012005
12. C. Sozzi et al., P4.1089 46th EPS Conference on Plasma Physics EPS 2019, Milan Italy
13. P. Platania et al, AIP Conference Proceedings 1689, 090010 (2015); https://doi.org/10.1063/1.4936547